Superexchange Interaction in Orbitally Fluctuating RVO_3

J.-S. Zhou and J. B. Goodenough
Texas Materials Institute, University of Texas at Austin, Austin, Texas 78712, USA

J.-Q. Yan
Ames Laboratory, Ames, Iowa 50011, USA

Y. Ren
Advanced Photon Source, Argonne National Laboratory, Argonne, Illinois 60439, USA
(Received 18 May 2007; published 8 October 2007)

Changes in pressure and magnetic field in the orbital and magnetic ordering temperatures of RVO_3 perovskites are reported; they reveal a competition between two magnetic orbitally ordered phases that have opposite preferences for the e-orbital component in the localized $^3T_{1g}$ ground state of the V^{3+} ion. This competition is shown to be biased by the $VO_{6/2}$ site distortion intrinsic to the orthorhombic structure. A remarkable enhancement of T_N with pressure is found where the competition leads to enhanced orbital critical fluctuations.

DOI: 10.1103/PhysRevLett.99.156401 PACS numbers: 71.70.Ej, 75.10.Dg, 75.30.Et, 75.50.Ee

The discussion of spin-spin interaction on the basis of the orbital status started in the 1950s [1]. Interest in orbital physics has been revived in recent years [2] in consideration of the possible dynamic interference between the orbital space and spin space as put forward in the Kugel-Khomskii Hamiltonian [3]. A near degeneracy of two orbital and spin ordered phases makes the orthovanadates a unique class of materials for this study. The RVO_3 (R = rare earth) family of perovskites are all orthorhombic with $Pbnm$ space group at room temperature. In this structure, the cooperative rotations of the $MO_{6/2}$ octahedra are accompanied by an intrinsic site distortion having two components, a splitting of the (M-O) bond lengths into long, medium, and short, with the long axis alternating between cubic [100] and [010] directions in the (001) planes [4] and a decrease in the 90° O-M-O bond angle α that subtends the orthorhombic b axis [5]. The first component can be described precisely by a mixing of the tetragonal Q_3 and orthorhombic Q_2 vibrational modes. These intrinsic site distortions vary with the R^{3+}-ion radius IR. In perovskites having an average bond length $\langle$M-O$\rangle \approx 2.0$ Å, an $IR \approx 1.11$ Å marks a magic size for the R^{3+} ion where the first component is a maximum and the second component sets in with increasing IR to lower the difference $(b - a)$ in lattice parameters until they cross [5]. The octahedral-site V^{3+} ions of the RVO_3 family have a localized-electron $^3T_{1g}$ ground state containing a major t^2 component of ^3F and a minor et component of ^3P parentage; the free-ion orbital angular momentum of the ^3F state is not fully quenched by the cubic crystalline field [6]. In $LaVO_3$, where the (V-O) bond lengths are all nearly equal [7], a $\lambda \mathbf{L} \cdot \mathbf{S}$ spin-orbit coupling may play an important role; but where the intrinsic site distortion creates three different (M-O) bond lengths as IR decreases, the $\lambda \mathbf{L} \cdot \mathbf{S}$ term becomes less important and the intrinsic site distortion of the (V-O) bond lengths, which reaches a maximum near $GdVO_3$, biases the orbital ordering to give a maximum orbital ordering temperature $T_{OO} > T_N$ [8]. An orbital-flipping transition at $T_{CG} < T_N$, found for $IR < 1.10$ Å, signals that there is a subtle competition between spin-orbital interaction and the intrinsic structural bias effect in the interval $T_{CG} < T < T_N$. Since the intrinsic structural bias can be modified by hydrostatic pressure as well as by the R^{3+}-ion radius, this competition can be shifted by applying pressure. We demonstrate in this Letter the influence on the orbital-ordering and flipping transitions of the intrinsic structural distortion by means of high-pressure experiments. Most importantly, whereas the discussion of the role of an orbital degree of freedom on the spin-spin interaction continues, no systematic study has been made to address what happens to the spin-spin interaction as the orbital-ordering status changes. The pressure-induced orbital-state changes near T_N in the RVO_3 family add a new component to a most active subject of spin-orbital interactions in strongly correlated systems.

All samples in this work were made with the melt-growth method in an infrared-heating image furnace [9]. We have chosen the perovskites RVO_3 (R = Ce, Pr, Eu, Gd, Dy, Y, and Lu) in this study in order to cover the evolution as a function of IR for all phase transitions. The samples have nearly perfect oxygen stoichiometry as checked by the measurement of thermoelectric power. Both ac and dc magnetic susceptibility under pressure were performed in homemade Be-Cu devices in which the miniature device for the dc magnetization fits into a commercial superconducting quantum interference device magnetometer. The structural studies under high pressure were carried out at room temperature in a diamond anvil cell mounted in a four-circle diffractometer.

We highlight several important features in Fig. 1 of the magnetization $M(T)$ under pressure for RVO_3. For $CeVO_3$, (a) the field-cool (FC) and zero-field-cool (ZFC) curves split at $T < T_N$; (b) an anomaly of $M(T)$ at T_t, defined as a minimum in the $dM(T)/dT$ curve that can be seen more clearly in the FC curve, enhances the split between the ZFC and the FC curves; (c) the split, while becoming smaller as temperature increases, redevelops at higher temperatures under pressure to persist to T_N; (d) T_N is very sensitive to pressure. For $PrVO_3$, (a) the FC and the ZFC curves are split at $T < T_N$, the split becoming more obvious at $T <$ 70 K; (b) the anomaly of $M(T)$ at T_t found in $CeVO_3$ disappears; (c) T_N is much less sensitive to pressure for this compound and the other heavier rare earths until $R =$ Tb; (d) no obvious split between the ZFC and FC curves was found at T_N for this compound and all members with smaller IR all the way to $R =$ Lu; therefore, only the ZFC curves are plotted to show the spin ordering at T_N. For $DyVO_3$, (a) transitions are evident at two temperatures, T_{CG} and T_{GC}, in addition to the one at T_N as temperature decreases; (b) the transitions at both T_{CG} and T_{GC} have a similar giant pressure coefficient, but of opposite sign; (c) a significantly high magnetization of the phase below T_{GC} indicates that the magnetic moment of the Dy^{3+} ion is involved in the transition. For $LuVO_3$, (a) the figure shows in detail how T_{CG} approaches T_N under pressure; (b) we can clearly track T_{OO} and its pressure dependence from the temperature dependence of the inverse magnetization since Lu^{3+} carries no moment. Interestingly, pressure reduces T_{OO}, but this pressure effect is extremely small. The same pressure dependence of T_{OO} was also observed for $EuVO_3$ and YVO_3.

As shown in Fig. 2, all pressure dependences of the transition temperatures follow a linear fitting well, and the coefficient $d\ln T_N/dP$ is mapped out as a function of IR in the top part of Fig. 3. Whereas T_N changes smoothly as a function of IR in the phase diagram, the pressure dependence $d\ln T_N/dP$ for the whole family of RVO_3 perovskites segregates sharply into three zones of IR, $IR <$ 1.09 Å, 1.09 Å $< IR <$ 1.19 Å, and $IR >$ 1.19 Å; the coefficient $d\ln T_N/dP$ changes discontinuously at these zone boundaries. In order to find the implication behind this striking curve of $d\ln T_N/dP$ versus IR, we have to study how the perovskite structure responds to the change of IR and to hydrostatic pressure.

Decreasing IR causes a continuous increase of the cooperative octahedral-site rotations in this orthorhombic perovskite structure; apparently the site rotations are not directly related to the abrupt change of $d\ln T_N/dP$ as a function of IR and the other phase transitions shown in Fig. 3. The intrinsic $VO_{6/2}$ site distortions in the $Pbnm$ perovskite structure must be considered. The type-G orbital ordering below T_{OO} enhances the intrinsic octahedral-site distortion and lowers the structure symmetry from $Pbnm$ to $P2_1$ [10]. Therefore, the structural bias is clearly the driving force for the maximum of T_{OO} at $IR \approx 1.11$ Å. Whereas the bulk modulus $B_0 \approx 200$ GPa, which is in line with other transition-metal oxide perovskites, changes smoothly as IR decreases, the pressure dependence of the factor $s \equiv 2(b-a)/(b+a)$ changes sign at $IR \approx 1.09$ Å and shows a minimum at $IR > 1.19$ Å. The ds/dP changing sign at $IR \approx 1.11$ Å is caused by the pressure-induced reduction of the intrinsic structural distortion in the $Pbnm$ perovskites [11]. Two IR values, 1.09 Å and 1.19 Å, also mark the boundaries where the coefficient $d\ln T_N/dP$ changes discontinuously. The importance of this structural study is that all abrupt changes in Fig. 3, the maximum of T_{OO} at $IR \approx 1.11$ Å and a jump of $d\ln T_N/dP$ at $IR >$ 1.19 Å, the termination of the orbital-flipping transition

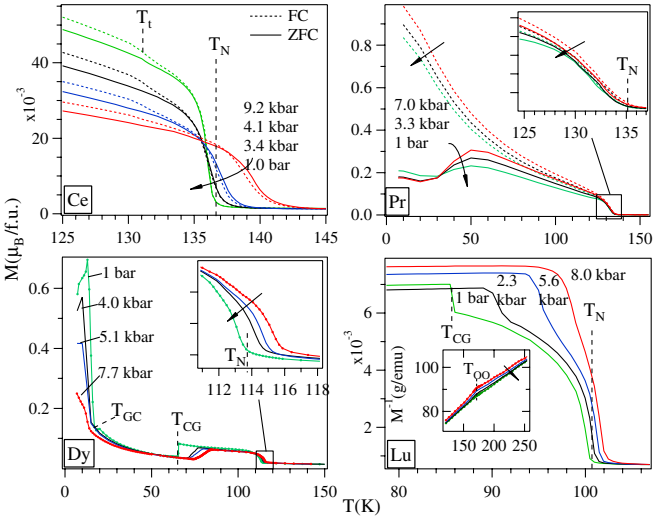

FIG. 1 (color online). Temperature dependences of the dc magnetization with 1 kOe magnetic field for the RVO_3 ($R =$ Ce, Pr, Dy, and Lu) under different pressures. Arrows point in the direction of decreasing pressure.

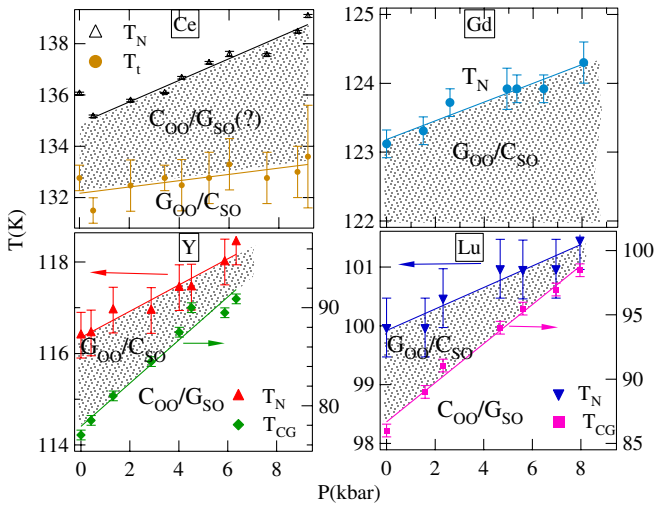

FIG. 2 (color online). Pressure dependences of the spin-ordering temperature T_N for the RVO_3 ($R =$ Ce, Gd, Y, and Lu), the orbital ordering temperature T_t for $R =$ Ce, and the orbital-flipping transition temperature T_{CG} for $R =$ Y and Lu.

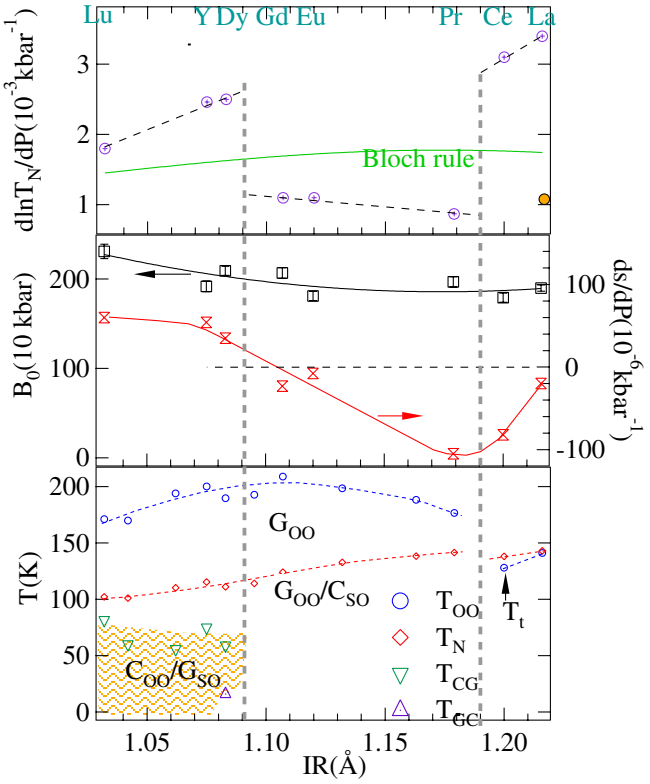

FIG. 3 (color online). Top: the IR dependence of the coefficient $d\ln T_N/dP$ for the RVO_3. T_N is determined in the ZFC measurement. The solid symbol for $LaVO_3$ is obtained in the FC measurement. Middle: the IR dependence of bulk modulus B_0 and the coefficient ds/dP for the RVO_3. Bottom: the phase diagram of transition temperatures versus IR for RVO_3, data from Ref. [8].

T_{CG}, and a drop of $d\ln T_N/dP$ at $IR \approx 1.10$ Å are all rooted in the intrinsic site distortions of the perovskite structure. Moreover, the bulk modulus B_0 obtained from this structural study under pressure provides a useful parameter to analyze the pressure dependence of T_N.

The empirical Bloch rule [12] $\alpha \equiv (d\ln T_N/dP)/\kappa \approx 3.3$ for a localized electronic state, where $\kappa = B_0^{-1}$ is the compressibility, serves as a benchmark for the volume dependence of T_N, where T_N increases under pressure with the gain in the orbital overlap integral. In Fig. 3 we have superimposed the curve of $d\ln T_N/dP$ versus IR calculated from the Bloch rule and the measured B_0. The $d\ln T_N/dP$ obtained for the RVO_3 perovskites that fall into the two IR zones $IR < 1.10$ Å and $IR > 1.19$ Å are significantly higher than those predicted by the Bloch rule. A possible cause for the unusually high $d\ln T_N/dP$ is that the crossover from localized to itinerant electronic behavior is approached from the localized-electron side as in $SmNiO_3$ [13]. However, this story is not applicable for the localized spins in the RVO_3 (R = Dy − Lu). We are forced to look at possible changes of the orbital state under pressure in addition to changes in the overlap-integral gain through shortening the bond length. This extra gain of T_N under pressure is turned off sharply for the phase in $1.10\text{Å} < IR < 1.19$ Å. In order to identify the possible mechanism responsible for the extra gain of T_N, we will elaborate the pressure effect on the structure and the structural evolution versus IR for these regions of IR. For $IR < 1.10$ Å, the orbitals undergo G-type ordering at T_{OO} and an orbital-flipping transition to C-type ordering at T_{CG}. In both types of orbital ordering, the long axis of the octahedra alternates direction within the (001) planes; there are changes from out-of-phase in the type-G to in-phase in type-C orbital order along the c axis and structural symmetry from $P2_1$ to $Pbnm$ [10,14]. Therefore, an abrupt volume change of the octahedra at T_{CG} cannot be explained by a simple switching from the in-phase to the out-of-phase configuration. The octahedral-site volume in the G_{OO} phase larger than that in the C_{OO} phase obtained from the structural studies [10] suggests a larger percentage of e orbital is present in the ${}^3T_{1g}$ ground state in the G_{OO} phase. More interestingly, the intrinsic component of the site distortion, which can be well-resolved in the orbitally disordered phase and in the G_{OO} phase, disappears in the C_{OO} phase of smaller volume where each $VO_{6/2}$ site has one long and two equally short V-O bonds. It is clear, therefore, that the orbital-flipping transition results from a competition between a spin-orbital interaction and the structural bias. Pressure favors the C_{OO} phase since it has a smaller cell volume and a smaller octahedral-site distortion, which explains the giant pressure dependence of T_{CG} in Fig. 2. As for the phase with $IR > 1.19$ Å, the orbital-ordering temperature T_t to the G_{OO} phase drops below T_N [8,15]. It is important to note that the G_{OO} phase with significant e-orbital occupation found in the region $IR < 1.11$ Å should be distinguished from the G_{OO} in $CeVO_3$ and $LaVO_3$ where pressure prefers slightly the G_{OO} over the orbitally disordered phase or the C_{OO} phase. This evolution of the G_{OO} phase reflects a crossover from a larger octahedral-site distortion that allows hybridization of t^2 and te configurations to a site symmetry that does not support this hybridization. Although the G_{OO} is found below T_{OO} for the phase with $IR < 1.19$ Å and below T_t for the phase with $IR > 1.19$ Å, the change from $dT_{OO}/dP < 0$ to $dT_t/dP > 0$ clearly supports the scenario of e-orbital occupation in the G_{OO} phase below T_{OO}. Since T_{CG} approaches T_N quickly under pressure for the region $IR < 1.10$ Å, this region and the region of $IR > 1.19$ Å share a common feature: there is an orbital-related transition in the vicinity below T_N. In contrast, the G_{OO} phase in the region from 1.11 to 1.19 Å is stable to lowest temperatures under the maximum pressure used in this study. Critical fluctuations are universally associated with an electronic phase transition; they affect physical properties such as transport properties [16] and thermal conductivity [17]. Therefore, orbital critical fluctuations associated with T_{CG} and T_t are likely to contribute a high $d\ln T_N/dP$ found in these two regions. The C_{OO} and G_{OO} phases are nearly degenerate in the vicinity of T_N in

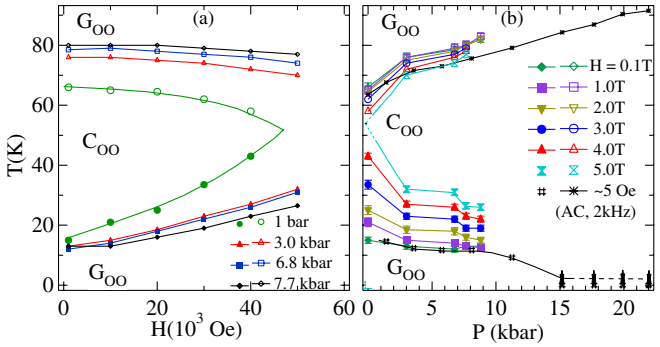

FIG. 4 (color online). (a) Magnetic-field dependence of orbital-flipping transitions T_{CG} and T_{GC} under different pressures for $DyVO_3$; (b) Pressure dependence of T_{CG} and T_{GC} under different dc magnetic fields and one ac field.

$LaVO_3$, which makes the pressure dependence of T_N highly sensitive to a ZFC versus a FC measurement [18].

The competition between the spin-orbital interaction and the structural bias effect can also be demonstrated by $DyVO_3$ with an IR near the magic value 1.11 Å, where the balance between these interactions is easily altered under a magnetic field and hydrostatic pressure. As shown in Fig. 1, there is an additional transition at $T_{GC} < T_{CG}$ in $DyVO_3$. Since the low-temperature phase below T_{GC} is suppressed under pressure, this orbitally ordered phase appears to be a reentry of the G_{OO} phase, which has been confirmed by diffraction with synchrotron radiation [19]. We show how T_{CG} and T_{GC} behave under a combination of magnetic field and pressure in Fig. 4. The temperature range where the C_{OO} phase is stabilized shrinks as the magnetic field H increases. The temperature range of the C_{OO} phase eventually disappears under $H = 5$ T; see Fig. 4(a). However, corresponding to the same magnetic field, the temperature range for the C_{OO} phase expands dramatically at a modest pressure $P = 3.0$ kbar, and this expansion continues as pressure increases further. The pressure effect can be shown more clearly in Fig. 4(b). T_{GC} is suppressed below 5 K under $P = 15$ kbar. The magnitudes of dT_{CG}/dP and dT_{GC}/dP are close to each other, which is consistent with a reentry of the G_{OO} phase at $T < T_{GC}$.

The bias effect from the intrinsic site distortion in the orthorhombic perovskite structure, which is a maximum at room temperature near $IR \approx 1.11$ Å, increases as temperature decreases. The spin-orbital interaction dominates in the C_{OO} phase so that the octahedral-site distortion characteristic of ordering t electrons into xy and yz (or zx) orbitals is observed. A reentry to the G_{OO} phase below T_{GC} indicates that the balanced competition shifts back to the side dominated by the structural bias. Moreover, the stronger spin canting in the G_{OO} phase relative to that in the C_{OO} phase, as seen in the magnetization measurements of Fig. 1, makes the G_{OO} phase more stable than the C_{OO} phase under a magnetic field. The new balance established on weighing between the structural bias and the magnetic-field effects on one side and the spin-orbital interaction on the other side is so subtle that even a modest pressure will break the balance and move the phase boundary T_{GC} to the lowest temperature.

In conclusion, the study of pressure effects on all phase transitions and on crystal structure for typical members of the RVO_3 perovskite gives three important results. (a) The orbital-flipping transition at T_{CG} from the G_{OO} to the C_{OO} and the reentry at T_{GC} are due to a competition between spin-orbital coupling and a strong bias from the intrinsic site distortion in the orthorhombic perovskite structure. The relatively strong spin canting in the G_{OO} phase makes it more stable under a magnetic field. On the other hand, pressure prefers the C_{OO} phase since it has the smaller cell volume than that of the G_{OO} phase. (b) The admixture of t and e orbitals in the G_{OO} phase for $IR < 1.10$ Å below T_{OO} makes the G_{OO} phase unstable under pressure relative to the orbitally disordered phase on one side and the orbitally ordered C_{OO} phase on the other side. (c) A much higher coefficient $d\ln T_N/dP$ than that predicted through a gain of the overlap integral is found where there is either an orbital-ordering transition at T_t or an orbital-flipping transition at T_{CG} right below T_N. Both T_{CG} and T_t increase under pressure. This observation suggests that orbital critical fluctuations in the vicinity of T_N are likely responsible for a new term in the spin-spin interaction that becomes manifest under pressure.

We thank R. J. McQueeney for his help to improve the manuscript and the Robert A. Welch Foundation and the NSF for financial support.

[1] J. B. Goodenough, Phys. Rev. **100**, 564 (1955).
[2] Y. Tokura *et al.*, Science **288**, 462 (2000).
[3] K. I. Kugel, D. I. Khomskii, Zh. Eksp. Teor. Fiz. **79**, 987 (1980), Sov. Phys. JETP **52**, 501 (1980).
[4] J.-S. Zhou *et al.*, Phys. Rev. Lett. **96**, 247202 (2006).
[5] J.-S. Zhou *et al.*, Phys. Rev. Lett. **94**, 065501 (2005).
[6] J. B. Goodenough, *Magnetism and the Chemical Bond* (Wiley, New York, 1963).
[7] P. Bordet *et al.*, J. Solid State Chem. **106**, 253 (1993).
[8] S. Miyasaka *et al.*, Phys. Rev. B **68**, 100406 (2003).
[9] J.-Q. Yan *et al.*, Phys. Rev. Lett. **93**, 235901 (2004).
[10] G. R. Blake *et al.*, Phys. Rev. Lett. **87**, 245501 (2001).
[11] J.-S. Zhou *et al.*, (unpublished).
[12] D. Bloch, J. Phys. Chem. Solids **27**, 881 (1966).
[13] J.-S. Zhou *et al.*, Phys. Rev. Lett. **95**, 127204 (2005).
[14] M. Reehuis *et al.*, Phys. Rev. B **73**, 094440 (2006).
[15] Y. Ren *et al.*, Phys. Rev. B **67**, 014107 (2003).
[16] G. A. Thomas *et al.*, Phys. Rev. Lett. **29**, 1321 (1972).
[17] H. Stern, J. Phys. Chem. Solids **26**, 153 (1965).
[18] J.-S. Zhou *et al.*, (unpublished).
[19] Y. Ren *et al.*, (unpublished).